Biosensors and Bioelectronics 55 (2014) 272–277

Contents lists available at ScienceDirect

Biosensors and Bioelectronics

journal homepage: www.elsevier.com/locate/bios

Electrochemical detection of Cu^{2+} through Ag nanoparticle assembly regulated by copper-catalyzed oxidation of cysteamine

Lin Cui [1], Jie Wu [1], Jie Li, Yanqiu Ge, Huangxian Ju *

State Key Laboratory of Analytical Chemistry for Life Science, Department of Chemistry, Nanjing University, Nanjing 210093, PR China

ARTICLE INFO

Article history:
Received 9 September 2013
Received in revised form
28 November 2013
Accepted 29 November 2013
Available online 17 December 2013

Keywords:
Electrochemical sensor
Copper-catalyzed cysteamine oxidation
Silver nanoparticles
Gold nanoparticles
Carbon nanotubes

ABSTRACT

A highly sensitive and selective electrochemical sensor was developed for the detection of Cu^{2+} by the assembly of Ag nanoparticles (AgNPs) at dithiobis[succinimidylpropionate] encapsulated Au nanoparticles (DSP-AuNPs), which was regulated by copper-catalyzed oxidation of cysteamine (Cys). The electrochemical sensor was constructed by layer-by-layer modification of glassy carbon electrode with carbon nanotubes, poly(amidoamine) dendrimers and DSP-AuNPs. In the absence of Cu^{2+}, Cys could bind to the surface of citrate-stabilized AgNPs via Ag–S bond, thus AgNPs could be assembled on the sensor surface through the reaction between DSP and Cys. In contrast, the copper-catalyzed oxidation of Cys by dissolved oxygen in the presence of Cu^{2+} inhibited the Cys-induced aggregation of AgNPs, leading to the decrease of the electrochemical stripping signal of AgNPs. Under the optimized conditions, this method could detect Cu^{2+} in the range of 1.0–1000 nM with a detection limit of 0.48 nM. The proposed Cu^{2+} sensor showed good reproducibility, stability and selectivity. It has been satisfactorily applied to determine Cu^{2+} in water samples.

1. Introduction

Copper is an essential micronutrient for biological functions and plays an important role in various physiological processes in organisms, including blood formation, connective tissue development, the functioning of a variety of metallo-enzymes and transcriptional events (Que et al., 2008). However, excessive intake of copper might produce reactive oxygen species (Strausak et al., 2001), and cause gastrointestinal disturbance, neurodegenerative diseases, and even damage to the liver and kidneys (Kim et al., 2009). The World Health Organization (WHO) has defined the maximum level of copper in drinking water at 2.0 ppm (30 nM). Thus, convenient and reliable copper detection methods are urgently needed in the fields of environment protection and human health (Zheng et al., 2007). Numerous analytical technologies have been developed for the detection of copper, such as atomic absorption spectroscopy (Faghihian et al., 2009), inductively coupled plasma mass spectrometry (ICP-MS) (Reddy et al., 2008), UV–vis spectroscopy (Zhang et al., 2010), colorimetric analysis (Zhou et al., 2008), chemiluminescence detection (Tang et al., 2005), and electrochemical techniques (Berchmans et al., 2008; Mülazımoğlu and Solak, 2011; Shao et al., 2012; Fu et al., 2013). Among these methods, electrochemical detection has attracted extensive attention due to their intrinsic advantages of simplicity, good portability, low cost, high sensitivity and selectivity.

Different modified electrodes have been reported to detect Cu^{2+} directly via stripping voltammetry, while most of them are interfered by other heavy metal ions and offer limited sensitivity (Oztekin et al., 2011; Flavel et al., 2011). Recently, a copper-catalytic alkyne–azide click reaction has been used to design highly sensitive electrochemical strategies for Cu^{2+} detection due to their high efficiency and good selectivity (Qiu et al., 2011a, 2011b). This method uses the azide modified electrode as a sensor and propargyl-functionalized ferrocene as electrochemical signal to detect Cu^{2+}. Although this method showed a very low detection limit down to fM level, it needs the pair of alkyne and azide groups as well as a reduction process of Cu^{2+} to Cu^{+}, which limits the real application of the click chemistry-based Cu^{2+} sensor.

Besides the click chemistry, Cu^{2+} can catalyze the oxidation of thiol compounds (R–SH) by O_2 to form disulfide compounds (R–S–S–R) (Pecci et al., 1997). Thus this reaction can regulate the assembly of metal nanoparticles induced by thiol compound. For example, 3-mercaptopropionic acid-induced agglomeration of DNA–Cu/Ag nanocluster has been used for sensitive fluorescence assay of Cu^{2+} (Su et al., 2010), and a colorimetric method has been developed for Cu^{2+} detection through L-cysteine-induced aggregation of gold nanoparticles (AuNPs) (Lu et al., 2012). This work used copper-catalyzed oxidation of cysteamine (Cys) to regulate

* Corresponding author. Tel.: +86 25 835 93593; fax: +86 25 359 3593.
E-mail address: hxju@nju.edu.cn (H. Ju).
[1] These authors contributed equally to this work.

0956-5663/$ - see front matter © 2013 Elsevier B.V. All rights reserved.
http://dx.doi.org/10.1016/j.bios.2013.11.081

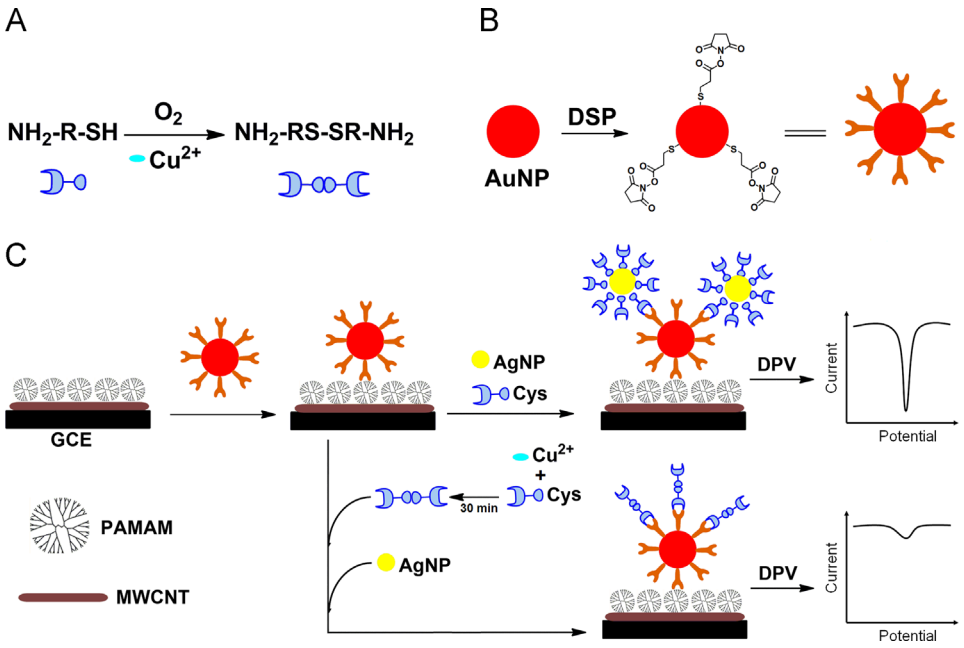

Scheme 1. Schematic diagram of (A) Cu^{2+}-catalyzed oxidation of Cys to disulfide cystamine by O_2, (B) preparation of DSP-AuNPs and (C) electrochemical detection of Cu^{2+}.

the assembly of Ag nanoparticles (AgNPs) at dithiobis[succinimidyl-propionate] encapsulated AuNPs (DSP-AuNPs) and design a sensitive sensor for selective stripping voltammetric detection of Cu^{2+}.

The sensor was prepared by layer-by-layer modification of glassy carbon electrode (GCE) with multi-walled carbon nanotubes (MWCNTs), poly(amidoamine) dendrimers (PAMAM) and DSP-AuNPs (Scheme 1). The DSP-terminated sensor could capture Cys functionlized AgNPs through the reaction between DSP and Cys. In the presence of Cu^{2+}, Cys was oxidized by dissolved oxygen to form cystamine, which was then bound to DSP-terminated sensor. Meanwhile, the formation of Cys functionlized AgNPs was blocked. The dual inhibition led to low loading of AgNPs on the DSP-terminated sensor, thus decreased the electrochemical stripping signal of AgNPs. Benefiting from the high catalytic activity of Cu^{2+} toward the oxidation of Cys, the proposed method showed good selectivity and easy operation. The presence of MWCNTs also promoted the electron transfer for anodic stripping of AgNPs, thus improved the sensitivity. The proposed sensor for Cu^{2+} showed excellent analytical performance and satisfactory results for water sample analysis.

2. Materials and methods

2.1. Materials and reagents

MWCNTs (CVD method, purity-98%, diameter 40–60 nm and length 1–2 μm) were purchased from Shenzhen Nanotech Port Co., Ltd. (Shenzhen, China). MWCNT was treated by ultrasonic in a 3:1 mixture (v/v) of concentrated H_2SO_4 and HNO_3 for 2 h, followed by a thorough washing with doubly distilled water until the filtrate reached neutral. After vacuum drying at room temperature, the MWCNT was dispersed in H_2O at a concentration of 0.1 mg mL^{-1}. Chloroauric acid ($HAuCl_4 \cdot 4H_2O$), trisodium citrate and silver nitrate ($AgNO_3$) were obtained from Shanghai Reagent Company (Shanghai, China). Cupric nitrate ($Cu(NO_3)_2 \cdot 3H_2O$) was purchased from Shanghai Sinpeuo Fine Chemical Co., Ltd. (China). Cys, PAMAM (ethylenediamine core, generation 5.0 solution, 5 wt% in methanol) and DSP were purchased from Sigma-Aldrich (St. Louis, MO). Other reagents were of analytical grade and used as received. Ultrapure water obtained from a Millipore water purification system (≥ 18 MΩ, Milli-Q, Millipore) was used in all assays.

2.2. Apparatus

All electrochemical experiments were performed with CHI660D electrochemical workstation (CH Instruments Inc., USA) with a conventional three-electrode cell, in which the bare or modified GCE (d=3 mm), saturated calomel electrode and platinum wire were served as the working, reference and auxiliary electrode, respectively. Electrochemical impedance spectroscopic (EIS) analysis was performed in 0.1 M KCl containing 5 mM $[Fe(CN)_6]^{3-}$/$[Fe(CN)_6]^{4-}$. The morphology of the AuNPs was examined using a JEM 2100 high-resolution transmission electron microscopic (TEM) (JEOL, Japan). Scanning electron microscopic (SEM) images were obtained by a Hitachi S-4800 scanning electron microscope (Japan). The UV–vis absorption spectra were obtained with a UV-3600 UV–vis–NIR spectrophotometer (Shimadzu Co., Kyoto, Japan). X-ray photoelectron spectroscopic (XPS) experiments were operated on an ESCALAB 250 spectrometer (Thermo-VG Scientific Co., USA) with an ultrahigh vacuum generator.

2.3. Preparation of DSP-AuNPs

AuNPs with 13 nm diameter were prepared by reducing $HAuCl_4$ with trisodium citrate according to the previous protocol (Cuquerella et al., 2011). The modification of Au-NPs with DSP through the ligand-exchange reaction was performed at room temperature by mixing 10 mL of the as-prepared AuNPs with 20 μL of 2 mM DSP aqueous solution (Kong et al., 2011). The mixture was treated ultrasonically in low modulate frequency over half an hour and incubated for 4 h at room temperature, which was then washed with centrifugation to remove the excessive DSP. The resulting DSP-AuNPs were washed with acetone twice and dispersed in deionized water. The dispersion was stored at 4 °C before use.

2.4. Preparation of AgNPs

AgNPs were prepared according to the reported work (Huang et al., 2008). In brief, 42.8 mL solution containing $AgNO_3$ (0.11 mM), sodium citrate (1.91 mM), PVP (0.052 mM) and H_2O_2 (25.0 mM) was prepared freshly. After $NaBH_4$ (150 μL, 100 mM) was added into the solution, its color turned to light yellow due to the chemical reduction of Ag^+ to produce AgNPs. Upon stirring for another 3 h, the AgNPs were collected by filtration with 0.2 μm membrane filters. The concentration of AgNPs was determined to be 0.1 μM with UV–vis spectroscopy.

2.5. Preparation of sensor

Firstly, the bare GCE was polished to mirror with 0.3 and 0.05 μm alumina slurry on micro-cloth pads. The electrode was sonicated in anhydrous ethanol and doubly distilled deionized water for 3 min, and dried with nitrogen. 5 μL of 0.1 mg mL^{-1} acid-treated MWCNT was then dropped onto the electrode surface. After the solvent was evaporated, the electrode surface was thoroughly rinsed with deionized water and dried in a nitrogen stream. Afterwards 5 μL of 0.5% PAMAM was coated on the electrode surface. After washing with water, DSP-AuNPs was deposited on the electrode by dropping 5 μL of the dispersion to obtain the sensor (DSP-AuNPs/PAMAM/MWCNT/GCE), which was stored at 4 °C prior to use.

2.6. Detection of Cu^{2+}

400 μL of Cu^{2+} solution or sample was mixed with 400 μL of 15 μM Cys in 100 mM pH 7.4 Tris–HCl buffer for 30 min to perform the catalytic oxidation of Cys by dissolved oxygen. Then, 200 μL of 0.1 μM AgNPs was added into the mixture and incubated for 10 min. After the sensor was immersed in the mixture and incubated for 30 min under stirring, differential pulse voltammetric (DPV) measurement was performed in 0.1 M Tris–HCl (pH 7.4) from 0 to 0.4 V at 100 mV s^{-1} to record the current response.

3. Results and discussion

3.1. Characterization of DSP-AuNPs and AgNPs

The morphology of AuNPs was investigated with TEM. It exhibited a uniform shape with an average diameter of 13 nm (Fig. 1A). This result was further confirmed by UV – vis spectrum in which an absorption peak was observed at 520 nm (Fig. 1B, curve a). The modification of AuNPs with small molecular DSP did not change their size. Both the TEM image (data not shown) and UV – vis spectrum of DSP-AuNPs (Fig. 1B, curve b) showed the size similar to AuNPs. Compared with the XPS spectrum of AuNPs, the XPS spectrum of DSP-AuNPs showed two new peaks at 162.8 and 401.8 eV (Fig. 1C and D), which corresponded to S_{2p} and N_{1s}, respectively. This result confirmed the successful modification of DSP on the AuNP's surface.

The TEM image of the synthesized AgNPs displayed high monodispersion, and their diameters were between 2 and 4 nm (Fig. 1E). In addition, the UV – vis spectrum of AgNPs exhibited a stable absorption peak at 406 nm (Fig. 1F), which corresponded to the typical absorption band of spherical AgNPs due to their surface plasmon.

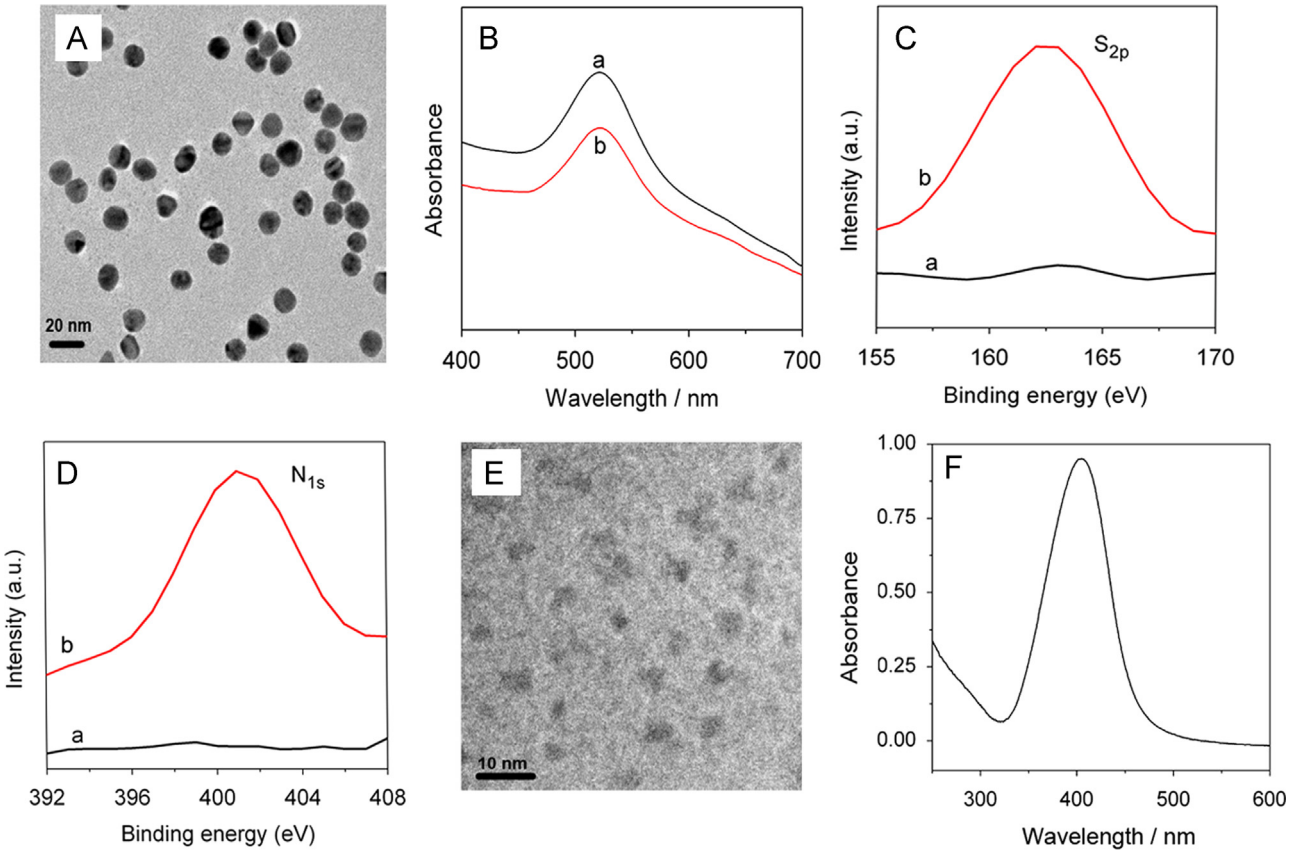

Fig. 1. (A) TEM image of AuNPs, (B) UV – vis absorption spectra and (C and D) XPS spectra of AuNPs (a) and DSP-AuNPs (b), (E) TEM image and (F) UV – vis absorption spectrum of AgNPs.

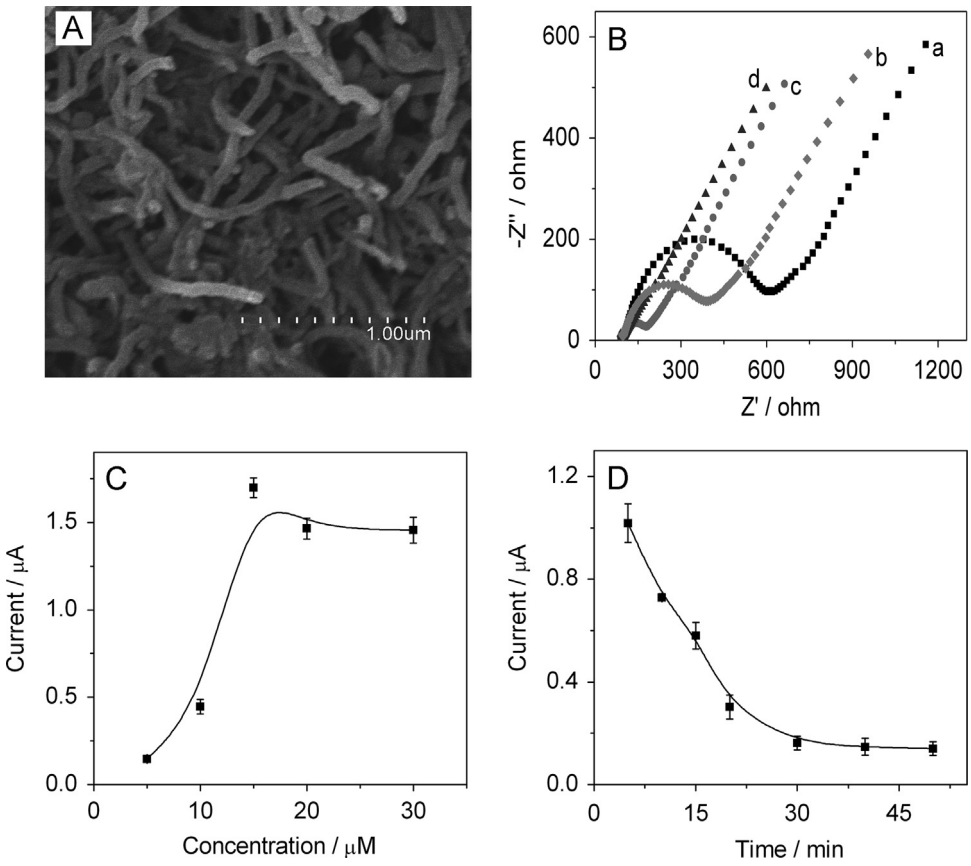

Fig. 2. (A) SEM image of acid-treated MWCNTs, (B) EIS of GCE (a), MWCNTs/GCE (b), PAMAM/MWCNTs/GCE (c) and DSP-AuNPs/PAMAM/MWCNT/GCE (d), and influences of (C) Cys concentration and (D) reaction time on stripping peak current.

3.2. Characterization of the chemical sensor

The sensor was constructed by layer-by-layer modification of MWCNTs, PAMAM and DSP-AuNPs on GCE. Before modification MWCNTs were treated with strong acid to obtain carboxylic groups. The SEM image of the carboxylated MWCNTs displayed a network of well-dispersed nanotube bundles (Fig. 2A), illustrating the integrity of the MWCNTs.

EIS measurements were performed in 0.1 M KCl containing 5 mM $[Fe(CN)_6]^{3-}$/$[Fe(CN)_6]^{4-}$ to examine the preparation process of the chemical sensor. In a typical EIS, the diameter of semicircle equals to the electron-transfer resistance, R_{et}, which reflects the electron transfer kinetics of the redox probe at the electrode surface. The MWCNT/GCE showed a much smaller R_{et} than bare GCE (Fig. 2B, curves a,b), implying that the carboxylated MWCNT was an excellent electric conducting material to accelerate the electron transfer. After the MWCNT/GCE was modified with PAMAM, a significant decrease in R_{et} was observed (Fig. 2B, curve c). This result could be attributed to the electrostatic attraction between negatively charged $[Fe(CN)_6]^{3-/4-}$ and positively charged PAMAM. After the additional modification with DSP-AuNPs, the R_{et} was further decreased, and the EIS of the sensor showed nearly a straight line (Fig. 2B, curve d), suggesting the successful conjugation of DSP-AuNPs on the surface of PAMAM/MWCNTs/GCE.

In order to evaluate the detection efficiency of the sensor, the DPV response of AgNPs loaded on the proposed sensor in the presence of 1.0 nM Cu^{2+} was compared those on DSP-AuNPs/GCE and DSP-AuNPs/PAMAM/GCE as controls. As shown in Fig. S1, the sensor showed much larger current than both DSP-AuNPs/GCE and DSP-AuNPs/PAMAM/GCE, suggesting MWCNTs accelerated the electron transfer efficiently and improved the sensitivity. Compared with the background, only the sensor showed obvious decrease of the stripping signal in the presence of Cu^{2+}, moreover, the presence of 10 nM interfering ions did not affect the signal change, indicating good specificity and detection selectivity.

3.3. Optimization of detection conditions

In present work, the detection of Cu^{2+} was based on the copper-catalyzed oxidation of Cys. As shown in Scheme 1, Cys could bind to the surface of AgNPs via Ag–S bond. The functionalized AgNPs could then be captured by the immobilized DSP-AuNPs through the reaction between the DSP and the amino group of Cys, which produced a high stripping voltammetric response of AgNPs. In the presence of Cu^{2+}, both the formation and the loading of Cys functionalized AgNPs on the DSP-terminated sensor were blocked due to the copper-catalyzed oxidation of Cys to produce cystamine, which could react with the DSP on sensor surface, leading to the decrease of stripping current of AgNPs. Thus, the relative concentration of Cys to AgNPs was extremely important for obtaining high detection efficiency. In this work, 0.1 μM AgNPs were used for all experiments, and the concentration of Cys was optimized at the fixed concentration of AgNPs. As shown in Fig. 2C, the stripping current increased gradually with an increasing Cys concentration and reached a plateau after a concentration of 15 μM. Thus, 15 μM of Cys was chosen for the subsequent experiments.

Fig. 2D displays the influence of reaction time for copper-catalyzed Cys oxidation on the stripping current. The peak current decreased significantly with the increasing reaction time, suggesting less AgNPs were captured on the sensor surface due to the formation of cystamine. The peak current decreased to a constant value after the reaction time of 30 min, indicating 30 min was

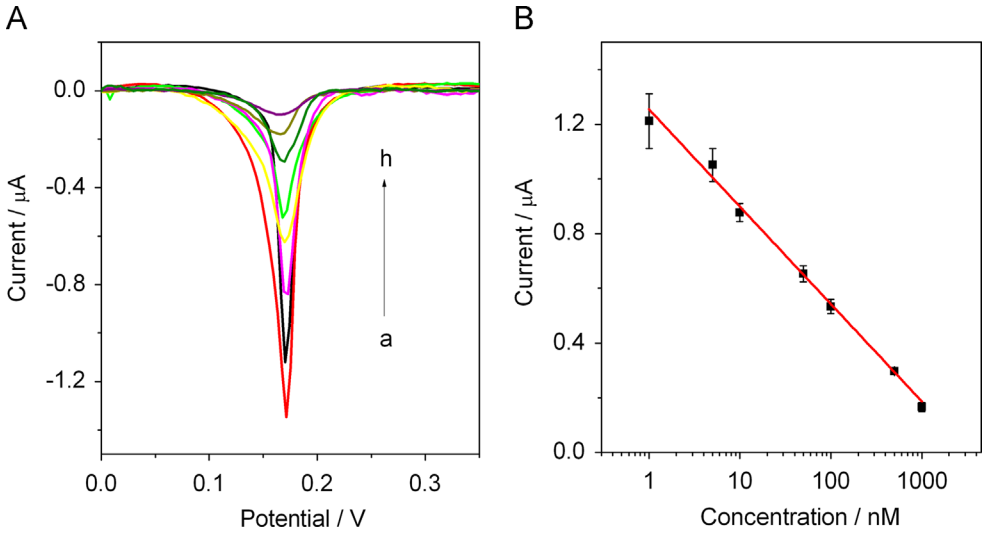

Fig. 3. (A) Differential pulse voltammograms at 0, 1.0, 5.0, 10, 50, 100, 500 and 1000 nM Cu^{2+} (from a to h), and (B) calibration curve for Cu^{2+} detection.

enough for the copper-catalyzed oxidation. Therefore, 30 min was selected as the optimal reaction time.

3.4. Detection of Cu^{2+}

Under the optimized conditions, Cys was reacted with different concentrations of Cu^{2+} for 30 min and subsequently incubated with AgNPs for a further 10 min. After the sensor was immersed in the mixture for 30 min to capture Cys–AgNPs, the peak current for electrochemical stripping of the loaded AgNPs decreased proportionally with the increasing concentrations of Cu^{2+} (Fig. 3A). The calibration plot showed a good linear relationship between the peak current and the logarithm value of Cu^{2+} concentration in the range of 1–1000 nM with a correlation coefficient of 0.9952 (Fig. 3B). The detection limit corresponding to a signal-to-noise ratio of 3 was 0.48 nM, which was much lower than the limit value of 20 nM in drinking water permitted by the U.S. EPA. In addition, the detection limit and sensitivity of the proposed method was much superior to other electrochemical Cu^{2+} detections by using catalytic DNA (Ocaña et al., 2013), polymer modified electrodes (Wang et al., 2011; Mülazımoğlu, 2012) and nanocomposite modified electrodes (Flavel et al., 2011; Liu et al., 2011; Ndlovu et al., 2012; Shao et al., 2012; Zhang et al., 2012). Compared with other copper-catalytic reaction based detection methods, this method did not need special reagents and/or additional reduction process for electrochemical detection, although AgNPs were needed to produce the anodic stripping signal, and the sensitivity and detectable range were also much better than those of colorimetric and fluorescent detection methods (Table S1).

3.5. Reproducibility, stability and selectivity

The reproducibility of the sensor was evaluated by determining the stripping current of AgNPs at 0.1 μM Cu^{2+} at 6 different sensors prepared independently. The relative standard deviation (R.S.D.) was found to be 4.8%, which indicated an acceptable reproducibility for sensor preparation. After the sensor was stored at 4 °C for 20 days, and it retained 92% of its initial response, indicating good stability of the sensor.

The selectivity of the proposed electrochemical detection strategy for Cu^{2+} was evaluated by challenging it with other environmentally relevant metal ions, including Mg^{2+}, Fe^{2+}, Hg^{2+}, Co^{2+}, Ni^{2+}, Zn^{2+}, Cd^{2+}, Pb^{2+}, Mn^{2+} and Al^{3+}. The experiment was performed by measuring the solution containing 0.1 μM of Cu^{2+} and 10 μM of the mentioned interfering ions. As shown in Fig. 4, the stripping peak currents in the presence of interfering ions were 87–113% of the peak current without interfering ion, indicating high selectivity for Cu^{2+} detection and potential application for analysis of complex samples. Interestingly, the presence of Mg^{2+}, Hg^{2+} and Al^{3+} decreased the response. This phenomenon might follow the Pearson hard–soft acid–base (HSAB) theory, in which Hg^{2+} is classified as soft acid and tends to bind preferentially with ligands containing S, whereas Al^{3+} and Mg^{2+}, classified as hard acids, prefer the coordination with RNH_2. So Hg^{2+} might compete with AgNPs to coordinate with Cys through Hg–S bond, and Mg^{2+} might coordinate with $-NH_2$ group of Cys to block the reaction between Cys and DSP-AuNPs. These interactions lowered the loading and stripping current of AgNPs.

3.6. Determination of Cu^{2+} in real samples

To demonstrate the application of the proposed approach, Cu^{2+} with known amount was spiked in tap and lake water. All the samples were filtered through a 0.2 μm membrane before detection. The results were shown in Table 1. The average recoveries ranged from 100.7% to 95.3% for three determinations, addressing good accuracy of the proposed method for Cu^{2+} detection in the real-world samples.

4. Conclusions

A novel electrochemical strategy was developed for highly sensitive and selective detection of Cu^{2+} by using copper-catalyzed oxidation of cysteamine to regulate the assembly of Ag nanoparticles on DSP-terminated sensor. The DSP-terminated sensor showed very low electron transfer resistance due to the presence of both MWCNTs and AuNPs, which greatly improved the sensitivity for stripping voltammetric detection of the loaded AgNPs. The open structure of AuNPs assembled on PAMAM/MWCNT modified GCE was favorable to the loading of AgNPs, leading to a wide linear range and high sensitivity. The high catalytic activity of Cu^{2+} toward the oxidation of Cys endowed the proposed method with good selectivity. The assay excluded the specific detection conditions needed in click chemistry-based assay. The sensor showed good reproducibility and stability and could determine Cu^{2+} in natural water sample with satisfactory

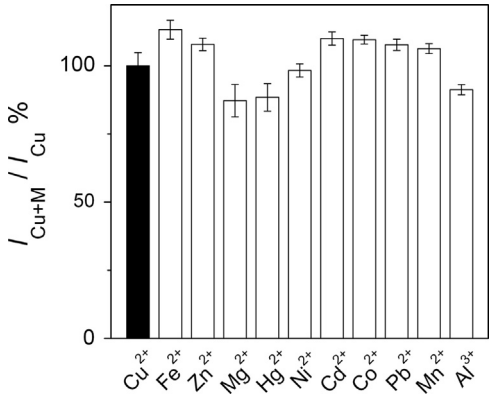

Fig. 4. Selectivity of the electrochemical sensor toward Cu^{2+}. I_{Cu} and I_{Cu+M} were the stripping peak currents for 0.1 μM Cu^{2+} solution and the mixture of 0.1 μM Cu^{2+} and 10 μM other metal ion, respectively.

Table 1
Determination of Cu^{2+} in water samples using the proposed method.

Sample	Added (nM)	Result (nM)	Recovery (%)
Tap water 1	10.0	9.50 ± 0.35	95.3
Tap water 2	50.0	48.79 ± 0.35	97.6
Lake water 3	100.0	98.57 ± 0.17	98.6
Lake water 4	200.0	201.44 ± 0.44	100.7

results, providing potential application in monitoring copper pollution samples in the environment.

Acknowledgments

We gratefully acknowledge the National Special Project for Key Scientific Apparatus Development (2012YQ170000302), National Basic Research Program (2010CB732400), National Natural Science Foundation of China (21105046, 21135002 and 21121091), PhD Fund for Young Teachers (20110091120012), and Natural Science Foundation of Jiangsu (BK2011552).

Appendix A. Supplementary material

Supplementary data associated with this article can be found in the online version at http://dx.doi.org/10.1016/j.bios.2013.11.081.

References

Berchmans, S., Vergheese, T.M., Kavitha, A., Veerakumar, M., Yegnaraman, V., 2008. Anal. Bioanal. Chem. 390, 939–946.
Cuquerella, M.C., Pocoví-Martínez, S., Pérez-Prieto, J., 2011. ChemPhysChem 12, 136–139.
Faghihian, H., Hajishabani, A., Dadfarnia, S., Zamani, H., 2009. Int. J. Environ. Anal. Chem. 89, 223–231.
Flavel, B.S., Nambiar, M., Shapter, J.G., 2011. Silicon 3, 163–171.
Fu, X.-C., Wu, J., Li, J., Xie, C.-G., Liu, Y.-S., Zhong, Y., Liu, J.-H., 2013. Sens. Actuators B: Chem. 182, 382–389.
Huang, T., Nallathamby, P.D., Xu, X.H.N., 2008. J. Am. Chem. Soc. 130, 17095–17105.
Kim, M.H., Jang, H.H., Yi, S., Chang, S.K., Han, M.S., 2009. Chem. Commun., 4838–4840.
Kong, B., Zhu, A., Luo, Y., Tian, Y., Yu, Y., Shi, G., 2011. Angew. Chem. 123, 1877–1880.
Liu, M., Feng, Y., Zhang, C., Wang, G., Fang, B., 2011. Anal. Methods 3, 1595–1600.
Lu, C.H., Wang, Y.W., Ye, S.L., Chen, G.N., Yang, H.H., 2012. NPG Asia Mater. 4, e10.
Mülazımoğlu, İ.E., 2012. Desalin. Water Treat. 44, 161–167.
Mülazımoğlu, İ.E., Solak, A.O., 2011. Anal. Methods 3, 2534–2539.
Ndlovu, T., Arotiba, O., Sampath, S., Krause, R., Mamba, B., 2012. Phys. Chem. Earth, 127–131.
Ocaña, C., Malashikhina, N., del Valle, M., Pavlov, V., 2013. Analyst 138, 1995–1999.
Oztekin, Y., Ramanaviciene, A., Ramanavicius, A., 2011. Sens. Actuators B: Chem. 155, 612–617.
Pecci, L., Montefoschi, G., Musci, G., Cavallini, D., 1997. Amino Acids 13, 355–367.
Qiu, S., Gao, S., Zhu, X., Lin, Z., Qiu, B., Chen, G., 2011a. Analyst 136, 1580–1585.
Qiu, S., Xie, L., Gao, S., Liu, Q., Lin, Z., Qiu, B., Chen, G., 2011b. Anal. Chim. Acta 707, 57–61.
Que, E.L., Domaille, D.W., Chang, C.J., 2008. Chem. Rev. 108, 1517–1549.
Reddy, D.K., Anil, G., Reddy, M., Mukkanti, K., Balaram, V., Rao, T.G., 2008. At. Spectrosc. 29, 201–209.
Shao, X., Gu, H., Wang, Z., Chai, X., Tian, Y., Shi, G., 2012. Anal. Chem. 85, 418–425.
Strausak, D., Mercer, J.F., Dieter, H.H., Stremmel, W., Multhaup, G., 2001. Brain Res. Bull. 55, 175–185.
Su, Y.T., Lan, G.Y., Chen, W.Y., Chang, H.T., 2010. Anal. Chem. 82, 8566–8572.
Tang, B., Niu, J., Yu, C., Zhuo, L., Ge, J., 2005. Chem. Commun., 4184–4186.
Wang, Z., Liu, X., Yang, J., Qin, Y., Lu, X., 2011. Electrochim. Acta 58, 750–756.
Zhang, J.F., Zhou, Y., Yoon, J., Kim, Y., Kim, S.J., Kim, J.S., 2010. Org. Lett. 12, 3852–3855.
Zhang, W., Wei, J., Zhu, H., Zhang, K., Ma, F., Mei, Q., Zhang, Z., Wang, S., 2012. J. Mater. Chem. 22, 22631–22636.
Zheng, N., Wang, Q., Zhang, X., Zheng, D., Zhang, Z., Zhang, S., 2007. Sci. Total Environ. 387, 96–104.
Zhou, Y., Wang, S., Zhang, K., Jiang, X., 2008. Angew. Chem. 120, 7564–7566.